Klein et al., J Nanomater Mol Nanotechnol 2014, S2
http://dx.doi.org/10.4172/2324-8777.S2-002

Journal of Nanomaterials & Molecular Nanotechnology

Research Article

A SCITECHNOL JOURNAL

# Oxidized Silicon Nanoparticles and Iron Oxide Nanoparticles for Radiation Therapy

**Stefanie Klein[1*], Anja Sommer[1], Maria L. Dell'Arciprete[2], Marc Wegmann[1], Susanne V. Ott[1], Luitpold V. R. Distel[3], Winfried Neuhuber[4], Mónica C. Gonzalez[2], and Carola Kryschi[2]**

## Abstract

Our research objective is to develop superparamagnetic iron oxide nanoparticles and silicon nanoparticles as radiosensitizers for cancer therapy. After internalization by breast tumor cells and irradiation with X-rays, the nanoparticles were observed to enhance the oxidative stress in tumor cells. While silicon nanoparticles increase the reactive oxygen species production under X-ray treatment due to their incompletely oxidized surface, positively charged amino-functionalized silicon nanoparticles enhance the formation of mitochondrial reactive oxygen species formation because of their direct interaction with the mitochondrial membrane. On the other hand, uncoated and citrate-coated superparamagnetic iron oxide nanoparticles were found to increase the reactive oxygen species formation in X-ray treated tumor cells via two particular surface features, being, first, the leakage of iron ions and second, the catalytic activity of nanoparticle surfaces. Both may initiate the Haber-Weiss and Fenton reaction.

## Keywords

Silicon nanoparticles; Superparamagnetic iron oxide nanoparticles; Radiation therapy; Reactive oxygen species generation

## Abbrevations:

IR: Ionizing Radiation, ROS: Reactive Oxygen Species, SiNPs: Silicon Nanoparticles, $NH_2$-SiNPs: Amino-silanized Silicon Nanoparticles, LT-SPIONs: Low Temperature Superparamagnetic Iron Oxide Nanoparticles, HT-SPIONs: High Temperature Superparamagnetic Iron Oxide Nanoparticles, TOAB : Tetraoctylammonium Bromide, APTES: Aminopropyltriethoxysilane, MCF-7: Human Breast Cancer Cells, DCF: 2',7'-Dichlorofluorescein, MMP: Mitochondrial Membrane Potential, MTT 3-(4,5-Dimethylthiazol-2-yl)-2,5-Diphenyltetrazolium Bromide

## Introduction

Radiation therapy is the medical use of low linear energy transfer ionizing radiation (IR) such as X-rays or γ-rays to kill malignant cells. IR may act directly on cellular material by either ionization or excitation, or indirectly via interactions with molecules by generating free radicals [1]. When water, the most abundant intracellular molecule, will be exposed to IR, decomposition reactions may occur, which generate a variety of reactive oxygen species (ROS) [2]. ROS are chemically reactive molecules that have essential functions in living organisms. A moderate increase in ROS can promote cell proliferation and differentiation [3,4], whereas excessive amounts of ROS cause oxidative damage to lipids, proteins, and DNA [5]. Because of the high proliferation rate of cancer cells and their reduced ability to repair DNA damage, IR has anticancer effects. Moreover, IR can be locally administered to a solid tumor, where it penetrates tissue and cellular boundaries.

However, there are various tumors that are hardly responsive to radiotherapy. One goal of radiotherapy is to enhance the radiotherapeutic efficacy for cancer to minimize its harmful effects on normal tissues. Therefore, radiosensitizers have been developed which increase the sensitivity of tumor cells to X-ray radiation [6]. Since ROS is a mediator to IR-induced cellular damage, generating further ROS by exogenous agents through irradiation can enhance the impact of radiotherapy. Promising radiosensitizers are noble metal and semiconductor nanoparticles. While for instance gold nanoparticles may increase the primary radiation damage via their emission of Compton electrons, photoelectrons or Auger electrons, semiconductor nanoparticles such as silicon or superparamagnetic iron oxide nanoparticles may increase the formation of ROS by interaction with X-rays via their surface.

In particular, surface-oxidized silicon nanoparticles (SiNPs) were reported to induce oxidative stress in a dose-dependent manner [7-9]. Radicals are evidently generated on surfaces of silica particles. Molecular oxygen reacts at the fractured silica surface, where both, homolytic ($Si^{\cdot}$, $SiO^{\cdot}$) and heterolytic ($Si^{+}$, $SiO^{-}$) cleavage of the silicon-oxygen bond takes place [10]. The mechanism of intracellular ROS generation in the presence of SiNPs involves both, the mitochondrial respiration and the NAD(P)H oxidase system [11,12]. A recent *in vitro* study revealed that surface-oxidized SiNPs smaller than 5 nm may increase the impact of X-ray irradiation on the ROS formation at clinically relevant doses. Furthermore, singlet oxygen was observed to be generated in X-ray treated solutions due to the presence of surface-stabilized silicon nanoparticles [13]. Coatings of SiNP surfaces with suited organic ligands were observed to suppress the silica-induced ROS generation and therefore is required for the development of biocompatible and biodegradable SiNPs for medical application [9]. SiNPs were functionalized with ethenyl derivatives that provide surface charges in aqueous environment due to their terminal amino ($NH_2$), azide ($N_3$), and carboxylic acid (COOH) groups [14]. In this context, the role of surface charges in cytotoxicity of such functionalized SiNPs was examined by Bhattacharjee et al. [15]. Positively charged SiNPs were observed to exhibit the highest cytotoxicity, since these SiNPs significantly increase the intracellular ROS production. One reason might be their interaction with mitochondrial membranes where they induce oxidative stress.

On the other hand, incompletely coated or uncoated superparamagnetic iron oxide nanoparticles (SPIONs) may promote the generation of ROS via different pathways. One occurs through the release of iron ions into the cytosol where immediate chelation by citrate or adenosine phosphate will take place [16-19]. Chelated iron ions can participate in the Haber-Weiss chemistry and thus, will catalyze the formation of the highly reactive hydroxyl radical that

***Corresponding author:** Dr. Stefanie Klein, Department of Chemistry and Pharmacy, Physical Chemistry I and ICMM, Friedrich-Alexander University of Erlangen-Nuremberg, Egerlandstr.3, D-91058 Erlangen, Germany, Tel: ++49 (0)9131 / 85-27508; Fax: ++49 (0)9131 / 85-28796; E-mail: stefanie.klein@fau.de

**Received:** April 25, 2014 **Accepted:** June 16, 2014 **Published:** June 20, 2014

damages cellular membranes, proteins and DNA. The other pathway involves SPION surfaces that may act as a catalyst for the Haber-Weiss and Fenton reaction. Voinov et al. [20] reported that -$Fe_2O_3$ nanoparticle surfaces catalyze the Haber-Weiss reaction in aqueous $H_2O_2$ solutions which starts via the superoxide-driven reduction of $Fe^{3+}$ to $Fe^{2+}$ and results in the formation of highly reactive hydroxyl radicals. They showed that surface $Fe^{3+}$ ions are at least 50-fold more efficient for the hydroxyl radical production than dissolved $Fe^{3+}$ ions. We are convinced that this catalytic effect of incompletely coated SPIONs has a promising potential for radiotherapy.

In this contribution, the cellular uptake and the influence of ultrasmall oxidized SiNPs, as well as amino-silanized oxidized SiNPs ($NH_2$-SiNPs) and citrate-coated and uncoated SPIONs on the cell viability and oxidative stress were studied. To examine the ability of different nanoparticles to function as radiosensitizers for X-rays, the coated and uncoated SiNPs or SPIONs were incubated with human breast cancer cells (MCF-7) that were subsequently irradiated. The radio-enhancement effect was assessed by measuring the intracellular ROS concentration.

## Materials and Methods

### Chemicals and instruments

Silicon tetrachloride (Aldrich, 99%), tetraoctylammonium bromide (TOAB, Aldrich, 98%), aminopropyltriethoxysilane (APTES, Aldrich, ≥ 98%,), lithium-aluminum hydride (Fluka, > 97%), toluene (VWR, 99.5%), cyclohexane (VWR, 100%), methanol (VWR, p. a.), $FeCl_3.6H_2O$ (99%, Acros organics), $FeCl_2 4H_2O$ (99%, Sigma-Aldrich) and citric acid anhydrous (99.5%, Alfa Aesar) were used as received. Dulbeco´s Modified Eagle Medium, L-glutamine, Fetal Calf Serum, penicillin-streptomycin-solution, sodium pyruvate, Phosphat Buffered Saline, MEM non-essential amino acid solution, trypsin/Ethylene Diamine Tetraacetic Acid, 3-(4,5-dimethylthiazol-2-yl)-2,5-diphenyltetrazolium bromide (MTT) (98%), trypan-blue-solution (0.4%), sodium dodecylsulfate (SDS) (90%), 2',7'-dichlorofluorescein diacetate (DCFH-DA) (95%) were purchased from Sigma-Aldrich and glutaraldehyde (25%) was bought from Roth. DCFH-DA was dissolved in dimethyl sulfoxide (DMSO) (99.7%, Baker) to obtain a stock solution (0.01 M) and was kept frozen at -20°C. For loading the cells with DCFH-DA the stock solution was mixed with DMEM to a final concentration of 100 µM.

The photoluminescence spectra of the DCF assay were recorded on a Horiba Jobin-Yvon FluoroMax-3 spectrofluorometer. The cells were imaged using a Zeiss 906 transmission electron microscope (LEO, Oberkochen, Germany). The concentrations of the nanoparticle sample solutions were determined using ICP-AES. The MTT assay was measured at 590 nm using an Elisa microplate reader (Dynatech Laboratories, Inc.). The different cells experiments were irradiated using a 120 kV X-ray tube (Isovolt, Seifert, Ahrensberg, Germany).

### Syntheses of SiNPs and $NH_2$-SiNPs

Silicon nanoparticles were synthesized using a reverse-micelle wet-chemistry procedure as previously reported by LLansola et al. [21]. 0.63 g of TOAB was dispersed for 20 min in toluene using an ultrasonication bath. 0.63 mL of $SiCl_4$ was pipetted into the solution and the sonication was maintained for 20 min. Then 0.76 g of $LiAlH_4$ was added to the solution. After 30 min of sonication, 30 mL of MeOH was slowly incorporated to the suspension to eliminate the excess of the reductant. In order to break the micelles, the mixture of solvents was evaporated and the particles were resuspended in 30 mL of cyclohexane. Three liquid-liquid extractions were performed with 30 mL of water. Finally, the organic phase was evaporated and the particles were resuspended in 20 mL of water for the cell experiments.

The functionalization of the SiNPs was performed via silanization. The toluene suspension of the SiNPs was stirred for 24 h at reflux with 1.5 mL of APTES. Afterwards, the suspension was evaporated and 20 mL of water was added. The purification of the functionalized SiNPs was performed via dialysis. The aqueous suspension was put into a Serva Membra-Cell MWCO 7000 membrane and the dialysis tube was submerged in distilled water. After the first 4 h, the water was changed twice and the suspension was left overnight. Finally, the suspension was evaporated and the $NH_2$-SiNPs were resuspended in water.

### Syntheses of SPIONs

There are two synthesis procedures applied here to prepare uncoated and citrate-coated SPIONs. One uses co-precipitation of ferric and ferrous chlorides in alkaline aqueous solution at low temperature (0°C) and follows Massart´s method [22]. The other consists of a high temperature one-pot synthesis in diethylene glycol (220°C) which is followed by alkaline co-precipitation and accomplished by a ligand exchange reaction step [23].

### Cell culture

The MCF-7 cells were cultured in DMEM containing 4500 mg glucose/L, which was enriched with 10% fetal calf serum (FCS), 1 mM sodium pyruvate, 100 U/mL penicillin, 100 µg/mL streptomycin, 2 mM L-glutamine and 1% MEM nonessential amino acids. In a humidified environment of 5% $CO_2$ the cells were incubated at 37°C and subcultivated twice a week.

### Transmission electron microscopy

MCF-7 cells were incubated with cell culture medium containing SiNPs and $NH_2$-SiNPs at a concentration of 0.1 mg Si/mL or SPIONs at a concentration of 0.1 mg Fe/mL. Cells were washed with PBS and fixed with 2.5% glutaraldehyde overnight at 4°C and then postfixed in 1% osmium tetroxide and 3% potassium ferricyanide at room temperature. Through graded alcohols cells were dehydrated, embedded in Epon and mounted on Epon blocks. Uncontrasted silver-grey ultrathin sections were imaged.

### Cell viability assay

Mitochondrial function and cell viability were evaluated using the MTT assay. The cells were seeded in a 96 well-plate at a density of $10^3$ cells per well for the experiments with the SPIONs and incubated for 3 days. Against it, the experiments with SiNPs were conducted with a cell density of $2\text{-}3*10^4$ cells per well and an incubation time of 24 h. For testing the cytotoxicity of the SiNPs the cell culture medium was replaced with one containing TOAB (0.1 mg/mL), APTES (0.1 mg/mL), SiNPs or $NH_2$-SiNPs both at a concentration of 0.1 mg Si/mL. In a second experiment the concentration of the SiNPs ranged from 10 to 75 µg Si/mL.

The viability of the citrate coated SPIONs was evaluated by replacing the cell culture medium with one containing SPIONs at a concentration of 0.1 mg Fe/mL. Thereby, control wells were left in medium without SPIONs. There were two samples created for the wells containing SPIONs, one to be used as sample well (containing nanoparticles and MTT solution) and one to serve as reference well

(containing nanoparticles, without MTT solution). The relative cell viability (%) was calculated by subtracting the absorbance of the reference well solution from that of the sample well solution and by subsequent division of the resulting difference in absorbance of the control well solution: $\{([A]_{sample}-[A]_{reference})/[A]_{control}\}\times 100$ where A refers to absorbance.

After 24 h, 48 h and 72 h incubation 50 µL of MTT solution (0.5 mg/mL in PBS) was added to each well. The solution was carefully removed after 1 h and the formazan crystals were solubilized with 100 µL DMSO. The cell viability was determined by measuring the absorbance of the formazan solution at 550 nm.

### Intracellular ROS measurement

MCF-7 cells were cultivated in 96 well-plates at a density of $10^3$ cells per well for the experiments with the SPIONs and were allowed to grow over 3 days. Also, the cells were seeded at a density of $2\text{-}3*10^4$ cells per well for the experiments with the SiNPs and incubated for 24 h. After removing the medium, the cells were incubated for 24 h with cell culture media that contains SiNPs (10, 50, 100 µg Si/mL), $NH_2$-SiNPs (0.1 mg Si/mL), SPIONs (0.1 mg Fe/mL) or iron salts (0.1 mg Fe/mL). Afterwards, the cells were washed with PBS and loaded with 100 µM DCFH-DA in DMEM. Following a 30 minute incubation time, each well was loaded with PBS. One half of the plate was irradiated at a single dose of 1 or 3 Gray (Gy). Due to the presence of ROS intracellular DCFH was oxidized to the fluorescent DCF dye. The DCF fluorescence intensity is directly proportional to the ROS concentration. The fluorescence emission was excited at 480 nm, and its spectrum was recorded in the range of 500 - 700 nm. Values of the relative fluorescence intensity were obtained by integrating the spectra. The obtained results of fluorescence intensities were related to those obtained from fluorescence measurements of cells in culture medium.

### Statistical analysis

Data are presented as arithmetic mean values ± standard error (SE). Statistical analysis was performed using the analysis of variance (ANOVA) with post hoc Bonferroni correction for multiple comparisons. A value of $p < 0.05$ was considered to be statistically significant.

## Results and Discussion

SiNPs, which were synthesized by a reverse micelle wet-chemistry procedure and subsequently functionalized with APTES via silanization, exhibit ultrasmall sizes around 1 nm. The cellular uptake of SiNPs and $NH_2$-SiNPs was verified upon TEM imaging of ultrathin sections of MCF-7 cells which had been incubated with medium containing these nanoparticles. There is no evidence for an uptake mechanism as being endocytosis or pinocytosis in any TEM micrographs for SiNPs or $NH_2$-SiNPs. Because of their ultrasmall sizes the SiNPs may directly cross the cell membranes by carriers,

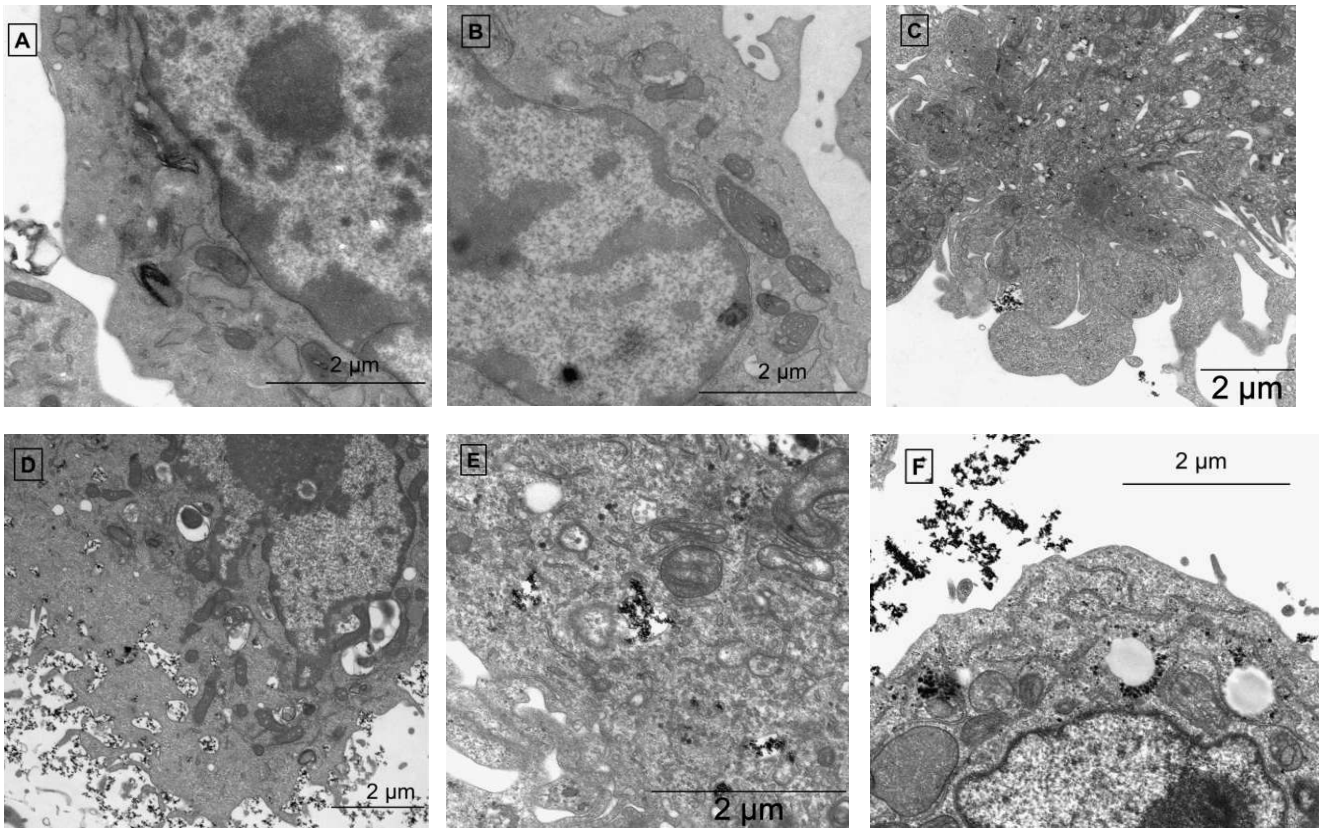


**Figure 1:** TEM images of MCF-7 cells incubated either with SPIONs or SiNPs: LT-SPIONs (A) as well as HTSPIONS (B) are taken up by endocytosis, transported in the endosomal pathway (C), and degraded in the lysosomes (D). $NH_2$-SiNPs incorporate in membranes of different cell structures (E). SiNPs agglomerate in the cytoplasm and in the membranes of cell organelles with at the same time reaching the cell nucleolus (F).

transporters or diffusion. The positively charged $NH_2$-SiNPs were found in the membranes of most cell structures such as endoplasmatic reticulum, mitochondria or vesicles (Figure 1A). Agglomerates of SiNPs were found in the cytoplasm, as well as in the membranes of cell organelles. Moreover, the SiNPs were observed being located in the cell nucleus, where they may damage the DNA (Figure 1B).

Citrate-coated SPIONs were obtained via two different synthesis routes. In the low temperature (LT) procedure SPIONs were obtained by co-precipitation of ferrous and ferric chloride in an aqueous ammonia solution at 0°C. Subsequently to several washing procedures the surfactant citric acid was added. The other procedure is a high temperature (HT) one-pot synthesis in diethylene glycol at 220°C followed by a ligand exchange reaction. The alkaline co-precipitation leading to seed formation and particle growth was stopped by adding the surfactant citric acid. The LT procedure yielded roughly spherical SPIONs with a relatively broad-size distribution between 6 and 20 nm, while the HT synthesis technique resulted in almost spherical SPIONs with sizes between 3 and 10 nm. The internalization of SPIONs by MCF-7 cells was illustrated by TEM images of these cells which had been incubated with SPIONs. In contrast to the SiNPs, the most probable entry mechanism for LT-SPIONs as well as the HT-SPIONs is endocytosis (Figure 1C and D), which is indicated by the formation of the pseudopodia towards the SPIONs. Afterwards, the nanoparticles can be found inside vesicles of the endosomal pathway (Figure 1E). As shown in Figure 1F the SPIONs accumulated around the membranes of lysosomes wherein their degradation should have taken place.

The biocompatibility of the obtained nanoparticles for the MCF-7 cells (Figure 2) was evaluated using the MTT assay. The relative cell viability (%) of the cells incubated with either SiNPs or $NH_2$-SiNPs was compared to medium containing APTES or TOAB (Figure 2A). The surfactant APTES (92%) has obviously no influence on the cells. In contrast, TOAB, that may form micelles during the synthesis, reduces the cell viability drastically. The detergent TOAB provides a higher permeability for the cell membrane which indispensably causes cellular damage. The SiNPs exhibit the lowest values of relative cell viability. Because of their cytotoxicity, the MTT assay with different SiNPs concentrations ranging from 10 to 75 µg Si/mL was carried out. Even the lowest concentrations of 10 µg Si/mL showed a low survival rate over the measured time period. Surprisingly the concentration of 50 µg Si/mL had the best biocompatibility (72%) for 24 h. The values decreased steadily for 48 and 72 h, but the survival rate was still above 50%. The cell viability of both 20 and 75 µg/mL was below 50% after 72 h. Due to their best biocompatibility the 10 and 50 µg Si/mL of SiNPs were used for the irradiation experiments. One reason for the cytotoxicity of the SiNPs is given by their small sizes that allow them to enter the nucleus within the first 24 h. In addition, the SiNPs are able to induce the formation of ROS. For instance, singlet oxygen, being generated in the nucleus, was reported to degrade guanine bases of the DNA [24]. In contrast, the $NH_2$-SiNPs are negligibly cytotoxic which is explained with their amino-silanized $SiO_x$ shell.

Figure 2C shows the cell viability of the cells incubated with uncoated and citrate-coated LT-SPIONS for the time period of 24 to 72 h, which was compared with cell culture medium containing citric acid. In case of the uncoated and citrate-coated LT-SPIONs the values of the cell survival ranges between 90 and 100% (Figure 2C). Very similar results were obtained for uncoated and citrate-coated HT-SPIONs (Figure 2D), whereas incubation in presence of citric acid was observed to result in a drastic reduction (Figure 2C and D).

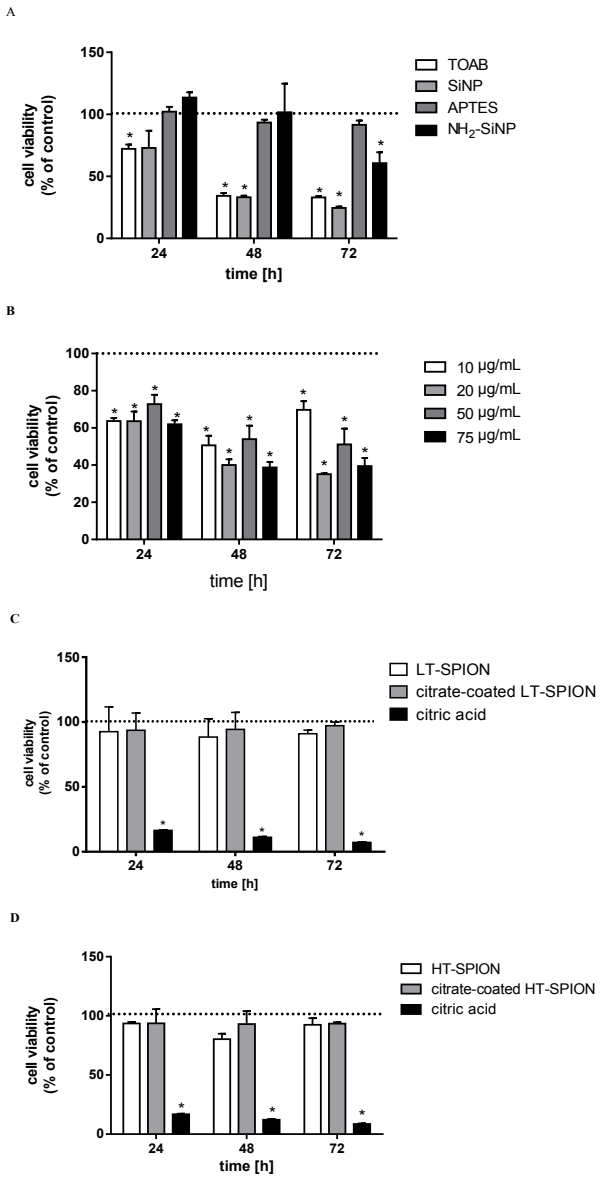


**Figure 2:** The biocompatibility of the SiNPs and SPIONs was tested using the MTT Assay: the metabolic activity (%) of MCF-7 cells loaded with TOAB, APTES, SiNPs or $NH_2$-SiNPs (A), examination of the concentration dependency of the SiNPs toxicity (B), MCF-7 cells loaded with citric acid, citrate-coated and uncoated LT-SPIONs (C) and HT-SPIONs (D), the dotted line refers to the control cells in medium, n = 6, *p > 0.05.

The cell number decreased in the presence of citric acid due to its use for detaching adherent cells like MCF-7. According to these results, LT- and HT-SPIONs exhibit an insignificant small influence on the cell viability of the examined cell line.

Our main objective was to quantitatively determine and elucidate the radio-enhancing effect of internalized nanoparticles. Since the X-ray treatment of tumor cells led to an enhanced formation of ROS, the ROS concentration of MCF-7 cells was determined to establish a probe for the effectiveness of intracellular nanoparticles. Therefore, MCF-7 cells were incubated with the different nanoparticles and

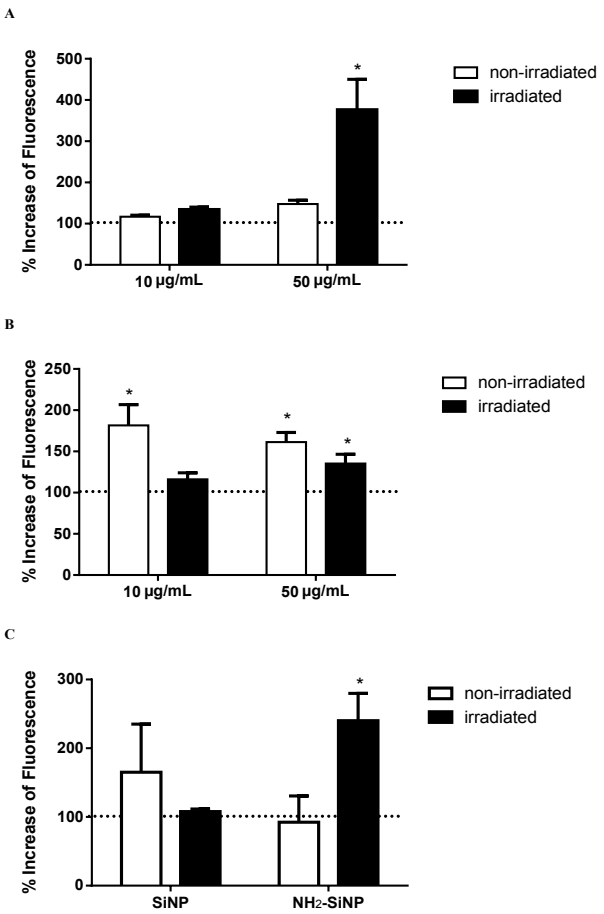


**Figure 3:** Determination of the relative ROS concentration in X-ray irradiated and non-irradiated MCF-7 cells loaded with SiNPs or $NH_2$-SiNPs. The value of the relative ROS concentration for MCF-7 are represented as increase of DCF fluorescence (%): irradiation of cells with SiNPs (10 and 50 µg/mL) at 1 Gy (A) and 3 Gy (B), and exposure of cells loaded with 100 µg/mL SiNPs and $NH_2$-SiNPs at 3 Gy (C), the dotted line refers to the control cells in medium, n = 6, *p > 0.05.

exposed to X-rays or left non-irradiated. The ROS concentration was measured via the fluorescence intensity of DCF that emerges due to quantitative oxidation of internalized non-fluorescent DCFH per mole ROS.

MCF-7 cells, loaded with 10 and 50 µg/mL SiNPs, were irradiated with a single dose of 1 and 3 Gy (Figure 3). At 1 Gy irradiation (Figure 3A) the lower concentration showed only a negligible increase of the ROS concentration (35%), whereas ROS generation in MCF-7 cells incubated with 50 µg/mL SiNPs raised drastically (276%). The incompletely oxidized surface of the SiNPs can induce the formation of singlet oxygen and possibly other ROS. This observation can be explained by unsaturated silicon atoms, that may possess either dangling bonds or are radicals itself. Another potential reason is based on the fact that $SiO_2$-particles may damage the mitochondrial membrane integrity and thereupon, cause a significant decrease of the mitochondrial membrane potential (MMP) [25]. The MCF-7 cells loaded with these nanoparticles and irradiated with 3 Gy (Figure 3B) were observed to exhibit a ROS concentration that is lower than that of non-irradiated cells. This result unambiguously confirms the cytotoxicity of the oxidized SiNPs. Presumably, the oxidized shell induces cell reactions that compete with or compensate the formation of ROS.

The completely oxidized and subsequently surface-functionalized $NH_2$-SiNPs cannot create ROS via their surface. However, under X-ray exposure with a single dose of 3 Gy $NH_2$-SiNPs were observed to increase the ROS concentration in MCF-7 cells for 180% (Figure 3C). It is well-established that X-rays induce the generation of free radicals in the cytoplasm. On the other hand, X-radiation also depolarizes the mitochondrial membrane and thereupon, may open the permeability transition pores and facilitate the cytochrome-c release to the cytoplasm. This release triggers the accumulation of ROS and increases the oxidation state of the cell. Also the inhibition of the respiratory chain raises the ubisemiquinone free radical level in the catalytic mechanism of complex III (ubiquinol/cytochrome-c oxidoreductase). The ubiquinone site in complex III appears as the major site of mitochondrial ROS production. It catalyzes the conversion of molecular oxygen to the superoxide anion radical by single electron transfer to molecular oxygen. The $NH_2$-SiNPs were observed to be embedded in the outer mitochondrial membrane, where they may enhance the impact of the X-rays on the mitochondria. This implies that the radiosensitizing effect of the $NH_2$-SiNPs mainly arises from their interaction with the mitochondria due to their location in the membrane.

Irradiation experiments were also carried out with coated and uncoated LT- and HT- SPIONs internalized by MCF-7 cells. All internalized SPION species resulted in increased ROS generation (Figure 4A). In particular, citrate-coated LT-SPIONs in X-ray treated MCF-7 cells enhanced the ROS formation by 240% when compared with X-ray treated cells without SPIONs. However, even LT-SPIONs in non-irradiated cells caused an increase of ROS concentration up to 77%. This implies that SPIONs do not only enhance the impact of X-rays on ROS formation but also may either act as catalysts via their surfaces or contribute to ROS formation with the release of iron ions. The latter effect arises from degradation of SPIONs when administrated into lysosomes where they are chelated by low molecular weight molecules. The iron ions may react via the Fenton or Haber-Weiss reaction with hydrogen peroxide and oxygen in the cytoplasm, which are released from the mitochondrial membrane as a by-product of the electron transport chain. To verify the contribution of intracellular iron ions (i.e. $Fe^{2+}$ and $Fe^{3+}$) to the ROS formation, MCF-7 cells were incubated with $Fe^{2+}$ or $Fe^{3+}$ solutions. The non-irradiated MCF-7 cells that contain iron ions exhibit relatively smaller ROS concentrations (Figure 4B) in comparison with the reference cells. X-ray exposure to these MCF-7 cells was observed to result in an increase of relative ROS concentration by 60 to 75%. For comparison, the value of relative ROS formation of X-ray exposed MCF-7 cells loaded with citrate-coated LT-SPIONs is 4-fold larger, whereas that of non-irradiated MCF-7 cells approximately reaches that of X-ray exposed MCF-7 cells containing iron ions. This implies that intracellular SPIONs may enhance the ROS formation due to the leakage of iron ions. Nevertheless, the larger contribution to the SPION-induced ROS formation arises from the catalytic activity of SPION surfaces which is quite enormous under X-ray exposure. We assume that X-radiation removes covalently bound and adsorbed surface molecules so that X-ray treated surfaces contain highly reactive $Fe^{2+}$ and $Fe^{3+}$ ions that may promote both, the Fenton and Haber-Weiss reactions. The relative content of $Fe^{2+}$ and $Fe^{3+}$ ions depend on the synthesis technique and subsequent surface stabilization method.

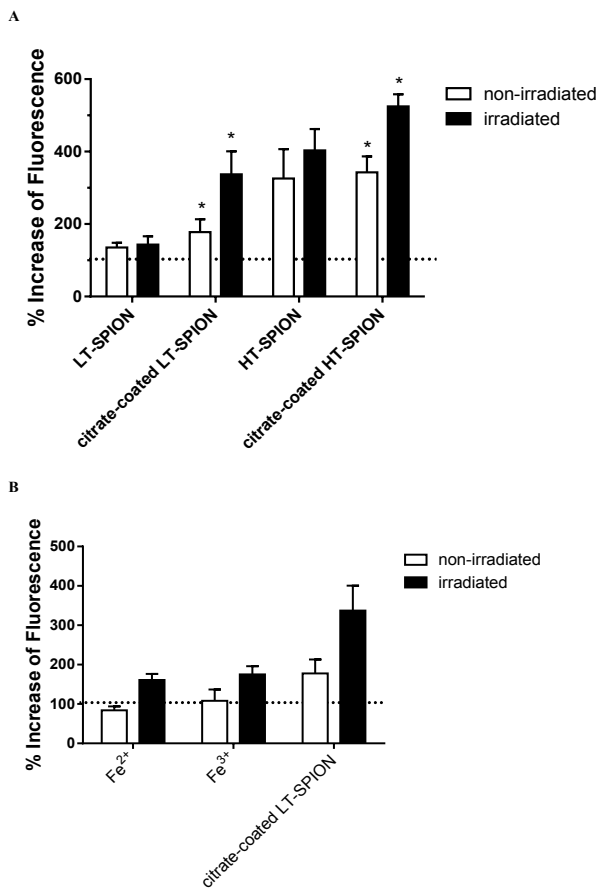


**Figure 4:** Determination of relative ROS concentration in X-ray irradiated and non-irradiated MCF-7 cells loaded with uncoated and citrate-coated LT- and HT-SPIONs (A) or loaded with $Fe^{2+}$, $Fe^{3+}$ or citrate-coated LTSPIONs (B) using the DCFH-DA assay: the values of relative ROS concentration are represented as increase of DCF fluorescence intensity (%), the dotted line refers to the control cells in medium, n = 6, *p > 0.05.

**Table 1:** Summary of the data of the cell viability assay after 24h of exposure to nanoparticles and of the ROS formation after X-radiation with 1 or 3 Gy for the different nanoparticles.

| Nanoparticle | Concentration [µg/ml] | Cell viability 24h [%] | ROS generation after irradiation [%] | |
|---|---|---|---|---|
| | | | 1 Gy | 3 Gy |
| SiNPs | 10 | 63.8 | 134.3 | 116.2 |
| | 50 | 72.8 | 376.2 | 135.2 |
| | 100 | 65.1 | -- | 107.8 |
| $NH_2$-SiNPs | 100 | 113.5 | -- | 240.1 |
| HT-SPIONs | 100 | 93.6 | -- | 403.1 |
| citrate-coated HT-SPIONs | 100 | 93.7 | -- | 524.7 |
| LT-SPIONs | 100 | 92.5 | -- | 143.2 |
| citrate-coated LT-SPIONs | 100 | 93.6 | -- | 337.3 |

The surface of LT-SPIONs predominantly consists of $Fe^{3+}$ ions that promote the Haber-Weiss reaction, whereas HT-SPION surfaces contain both, the $Fe^{2+}$ and $Fe^{3+}$ ions, and thereupon may catalyze the Fenton as well as the Haber-Weiss reaction. This hypothesis is consistent with the observation that uncoated and citrate-coated HT-SPIONs in non-irradiated MCF-7 cells led to largest values of relative ROS concentration (Figure 4A). The exposure of the SPION loaded MCF-7 to X-rays resulted in an additional increase of the ROS concentration. This is explained with the impact of high-energy X-rays on the SPION surfaces. The surface coverage consisting of either adsorbed citrate molecules, water or hydroxyl ions were partially destroyed during the X-ray exposure. The freed surface structures contain easier accessible iron ions that may exhibit a larger catalytic effect on the ROS production.

In summary, the uncoated or citrate-coated SPIONs and $NH_2$-SiNPs showed a good biocompatibility for the MCF-7 cells. Cells loaded with these nanoparticles generated more ROS after irradiation at 3 Gy and therefor, could be used as radiosensitizers. In contrast, the SiNPs are cytotoxic, and only very small concentrations could be used for the irradiation experiments. However, these small amounts of incorporated SiNPs enhanced effectively the formation of ROS at a single dose of 1 Gy. These conclusions are substantiated by the experimental data listed in table 1.

## Acknowledgements

Support of the Deutsche Forschungsgemeinschaft (graduate school 1161/2) is gratefully acknowledged. We thank Andrea Hilpert for TEM imaging studies (Institute of Anatomy I, University Erlangen-Nuremberg). Furthermore, we are grateful to Andreas Postatny for conducting so diligently the ICP-AES experiments on our samples. (Prof. Dr. Peter Wasserscheid, Institute of Chemical Reaction Technique, University Erlangen-Nuremberg).

## References

1. Bischoff P, Altmeyer A, Dumont F (2009) Radiosensitising agents for the radiotherapy of cancer: advances in traditional and hypoxia targeted radiosensitisers. Expert Opin Ther Pat 19: 643-662.
2. Hosoki A, Yonekura S, Zhao QL, Wei ZL, Takasaki I, et al. (2012) Mitochondria-targeted superoxide dismutase (SOD2) regulates radiation resistance and radiation stress response in HeLa cells. J Radiat Res 53: 58-71.
3. Boonstra J, Post JA (2004) Molecular events associated with reactive oxygen species and cell cycle progression in mammalian cells. Gene 337: 1-13.
4. Schafer FQ, Buettner GR (2001) Redox environment of the cell as viewed through the redox state of the glutathione disulfide/glutathione couple. Free Radic Biol Med 30: 1191-1212.
5. Perry G, Raina AK, Nunomura A, Wataya T, Sayre LM, et al. (2000) How important is oxidative damage? Lessons from Alzheimer's disease. Free Radic Biol Med 28: 831-834.
6. Juzenas P, Chen W, Sun YP, Coelho MA, Generalov R, et al. (2008) Quantum dots and nanoparticles for photodynamic and radiation therapies of cancer. Adv Drug Deliv Rev 60: 1600-1614.
7. Ahmad J, Ahamed M, Akhtar MJ, Alrokayan SA, Siddiqui MA, et al. (2012) Apoptosis induction by silica nanoparticles mediated through reactive oxygen species in human liver cell line HepG2. Toxicol Appl Pharmacol 259: 160-168.
8. Lin W, Huang YW, Zhou XD, Ma Y (2006) In vitro toxicity of silica nanoparticles in human lung cancer cells. Toxicol Appl Pharmacol 217: 252-259.
9. Morishige T, Yoshioka Y, Inakura H, Tanabe A, Yao X, et al. (2010) The effect of surface modification of amorphous silica particles on NLRP3 inflammasome mediated IL-1beta production, ROS production and endosomal rupture. Biomaterials 31: 6833-6842.
10. Fubini B, Hubbard A (2003) Reactive oxygen species (ROS) and reactive nitrogen species (RNS) generation by silica in inflammation and fibrosis. Free Radic Biol Med 34: 1507-1516.
11. Kim KA, Kim YH, Seok Seo M, Kyu Lee W, Won Kim S, et al. (2002) Mechanism of silica-induced ROS generation in Rat2 fibroblast cells. Toxicol Lett 135: 185-191.
12. Deshpande A, Narayanan PK, Lehnert BE (2002) Silica-Induced Generation of Extracellular Factor(s) Increases Reactive Oxygen Species in Human Bronchial Epithelial Cells. Toxicol Sci 67: 275-283.
13. Gara PMD, Garabano NI, Portolés MJL, Moreno MS, Dodat D, et al. (2012) ROS enhancement by silicon nanoparticles in X-ray irradiated aqueous suspensions and in glioma C6 cells. J Nanopart Res 14: 741.

14. Ruizendaal L, Bhattacharjee S, Pournazari K, Rosso-Vasic M, de Haan LHJ et al. (2009) Synthesis and cytotoxicity of silicon nanoparticles with covalently attached organic monolayers. Nanotoxicology 3: 339-347.

15. Bhattacharjee S, de Haan LHJ, Evers NM, Jiang X, Marcelis AT et al. (2010) Role of surface charge and oxidative stress in cytotoxicity of organic monolayer-coated silicon nanoparticles towards macrophage NR8383 cells. Part Fibre Toxicol 7: 25.

16. Auffan M, Achouak W, Rose J, Roncato MA, Chanéac C, et al. (2008) Relation between the redox state of iron-based nanoparticles and their cytotoxicity toward Escherichia coli. Environ Sci Technol 42: 6730-6735.

17. Nel A, Xia T, Mädler L, Li N (2006) Toxic potential of materials at the nanolevel. Science 311: 622-627.

18. Emerit J, Beaumont C, Trivin F (2001) Iron metabolism, free radicals, and oxidative injury. Biomed Pharmacother 55: 333-339.

19. Mahmoudi M, Simchi A, Imani M, Shokrgozar MA, Milani AS, et al. (2010) A new approach for the in vitro identification of the cytotoxicity of superparamagnetic iron oxide nanoparticles. Colloids Surf B Biointerfaces 75: 300-309.

20. Portolés MJL, Diez RP, Dell'Arciprete ML, Caregnato P, Romero JJ et al. (2012) Understanding the parameters affecting the Photoluminescence of Silicon Nanoparticles. J Phys Chem C 116: 11315-11325.

21. Massard R (1981) Preparation of aqueous magnetic liquids in alkaline and acidic media. IEEE Trans Magn 17: 1247-1248

22. Qu H, Caruntu D, Liu H, O'Connor CJ (2011) Water-dispersible iron oxide magnetic nanoparticles with versatile surface functionalities. Langmuir 27: 2271-2278.

23. Low SP, Williams KA, Canham LT, Voelcker NH (2010) Generation of reactive oxygen species from porous silicon microparticles in cell culture medium. J Biomed Mater Res A 93: 1124-1131.

24. Zhang Y, Hu L, Yu D, Gao C (2010) Influence of silica particle internalization on adhesion and migration of human dermal fibroblasts. Biomaterials 31: 8465-8474.

25. Fleury C, Mignotte B, Vayssière JL (2002) Mitochondrial reactive oxygen species in cell death signaling. Biochimie 84: 131-141.

## Author Affiliations

Top

[1]*Department of Chemistry and Pharmacy, Physical Chemistry I and ICMM, Friedrich-Alexander University of Erlangen-Nuremberg, Egerlandstr.3, D-91058 Erlangen, Germany*

[2]*Instituto de Investigaciones Fisicoquímicas Teóricas y Aplicadas (INIFTA), Facultad de Ciencias Exactas, Universidad Nacional de La Plata, Casilla de Correo 16, Sucursal 4, (1900) La Plata, Argentina*

[3]*Department of Radiation Oncology, Friedrich-Alexander University of Erlangen-Nuremberg, Universitätsstr. 27, D-91054 Erlangen, Germany*

[4]*Department of Anatomy, Chair of Anatomy I, Friedrich-Alexander University of Erlangen-Nuremberg, Krankenhausstr. 9, D-91054 Erlangen, Germany*



This article was originally published in a special issue, **Proceedings of the 5th International BioNanoMed 2014 Congress.**